A Real-Time DSP-Based Imbalance Analysis System for Rotating Machine with Vibration Signal

Hua Su, Linglong Huang, Kil To Chong*

Department of Electrical and Computer Engineering, Chonbuk National University, 664-14 Duckjin-Dong, Duckjin-Gu, Jeonju 561-756, Korea

This paper describes a new digital signal processor (DSP) imbalance measurement system dedicated to real-time vibration analysis on rotating machine. To accomplish real-time analysis, the vibration signals are on-line acquired and processed to analyze the mass imbalance and phase position. This is achieved through the use of FFT and Lissajous diagram. The method followed to analyze the mass imbalance with the chosen hardware and software solutions are described in detail in this paper. Several experimental tests demonstrate the efficiency and accuracy in imbalance analysis performance of the DSP system.

Key Words : Digital Signal Processor, Mass Imbalance, FFT, Lissajous Diagram

1. Introduction

Rotating machine is an excellent means for kinetic energy storage for electromagnetic launch applications due to high energy density available in spinning rotor and flywheels. The imbalance of rotor considered does not only cause vibration, it also transmits rotational force to the rotating machine and to the supporting structure. The forces thus transmitted may damage the machine and shorten its working life (Shin and Lee, 1997). Very often, imbalance results very dangerous damage in rotating machine, which can lead to a catastrophe. Actually, there have been many reports to these disasters (Park, 2000; Hoextermann,1988). Thus, it is necessary to develop a real-time system to identify the imbalance and its phase position, as efficiently as possible, to keep the stability of a system, to guarantee the safety for the men and to save the running cost.

* Corresponding Author,
E-mail : kitchong@chonbuk.ac.kr
TEL : +82-63-270-2478; **FAX** : +82-63-270-2451
Department of Electrical and Computer Engineering, Chonbuk National University, 664-14 Duckjin-Dong, Duckjin-Gu, Jeonju 561-756, Korea. (Manuscript **Received** October 28, 2004; **Revised** April 13, 2005)

Over the years, several methods have commonly been employed. The modal balancing technique was developed and further investigated by several researchers (Bishop and Gladwell, 1959; Shimada and Miwa, 1980; Saito and Azuma, 1964; Kim and Yoo, 2002), but with such method, the critical speed mode shape of the rotor must be known in advance, and mass distribution determined from the geometry of the rotor is not accurate. In additional, the finite element method (FEM) played an important role in the analysis of rotating machine due to its usefulness in vibration diagnosis (Park and Choi, 2004; Kim et al., 2003). However, there remain some difficulties in the computational aspect of imbalance analysis due to its inconvenient classical modal and complicated dynamics properties, such as rotational speed dependency and anisotropy (Hong and Park, 1997; Choi, 2003). Furthermore, various field imbalance analysis methods have also been developed and discussed (Enrich, 1987; Tahk and Shin, 2002; Hong and Seo, 2001).

In this paper, a DSP-based imbalance analysis system for real-time rotating machine imbalance diagnosis is designed and realized. A practical imbalance analysis approach recently proposed by the authors is implemented with customized software (Su and Chong, 2004). It is based on the

FFT and Lissajous diagram of analyzing the vibration spectra with statistical method. The vibration signal and reference time signal are obtained through the sensors on the rotor, and by transforming the vibration signal into its spectrum with FFT, the imbalance can be distinguished by the proposed DSP system. The phase position can then be located by computing the Lissajous diagram with the combined uses of the vibration signal and reference time signal after DSP processing. Real-time analysis is achieved because the computational time is drastically reduced by the proposed imbalance analysis approach and customized DSP system.

In the following, the approach used for imbalance identification is briefly described. Then the designed DSP system is presented, detailing both in hardware and software characteristics. Finally, several experimental tests are also conducted to validate the efficiency and applicability of the proposed DSP system.

2. Estimation of Imbalance

2.1 Estimation of mass imbalance

An imbalance causes a high intensity radial vibration at its rotation speed f_r, and the effect on the spectrum is a remarkable increase in the amplitude of the tone at f_r. For the practical imbalance distribution of a rotor, convergence conditions (Wylie and Barrett, 1982) are always satisfied and would not cause any convergence problem. This, the imbalance distribution should converge at some point of the rotor. In this paper, the work focuses on the efficient estimation of the equivalent imbalance and phase position of such point with the designed DSP system. We find that the amplitude of the vibration can reveal the imbalance, making it possible to estimate the imbalance by analyzing the amplitude of vibration spectra. The amplitude of vibration signal on frequency domain $V(f)$ is obtained by,

$$V(f)=FFT\{V_{DS}(t)\} \tag{1}$$

where $V_{DS}(t)$ is the vibration signals after down-sampling. Each value displays the energy of harmonics. Let us use the M_f as an estimate of the imbalance amplitude of the vibration sprctrum, then,

$$M_f=\max\{V(f)\,|\,f\subset B_r\} \tag{2}$$

where B_r is the frequency band of rotor rotation speed $[f_r-\delta, f_r+\delta]$ and δ is the frequency correction factor which will be explained in further detail later. The maximum value reveals the imbalance, in comparison with unit mass amplitude M_{UNIT} which is defined in advance through the experiment. The weight of mass imbalance can be shown as,

$$W=M_f/M_{UNIT} \tag{3}$$

There is an inaccurate problem deriving from the FFT method, which results in the spectral leakage (Blasco et al., 1996). The spectral leakage causes the spreading of the energy distribution of each harmonic. To reduce this problem, windowing must be applied to sampled time data. In this paper, the Hanning window is used, and defined as,

$$W(n)=0.5-0.5\cos(2\pi n/N+1) \tag{4}$$

where n is taken from 0 to N in each case. Thus, the new spectral of vibration signal $V_W(f)$ is expressed as,

$$V_W(f)=FFT\{V_W(t)\}=V_{DS}(f)*W(f) \tag{5}$$

where $V_W(f)$ is the windowed vibration signals in time domain. As the digital signal processor is applied in the proposed system, the discrete form of Eq. 5 is used. Due to the spectral leakage, the interpolation for the frequency of amplitude is also needed. Spectral leakage causes the spreading of the energy distribution of each harmonic. This results in a number of spectral lines for each harmonic as illustrated in Fig. 1. Letting the highest peak be at the i-th value with a magnitude v_i and defining a parameter r as,

$$r=\frac{v_i}{\max(v_{i+1},\ v_{i-1})} \tag{6}$$

then interpolation involves calculating a frequency correction factor δ so that the improved peak position is $f(v_i)+\delta$, where $f(v_i)$ is the frequency of magnitude v_i. The correction factor is a function of parameter r which depends on the

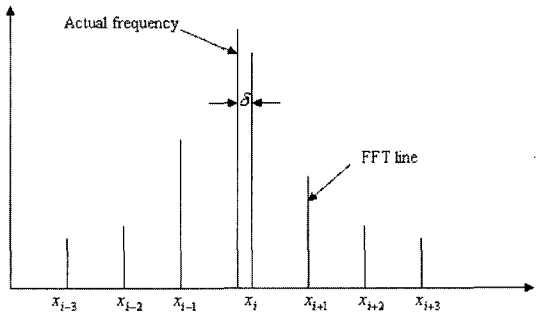

Fig. 1 Principle of spectra leakage and interpolation

data window being used. The general relationship between δ and r is obtained from the solution of,

$$0=\delta\sum_{m=0}^{N/2}\frac{(-)^m a_m}{\delta^2-m^2}-r(\delta-1)\sum_{m=0}^{N/2}\frac{(-1)^m a_m}{(\delta-1)^2-m^2} \quad (7)$$

where a_m are the weighting coefficients of the data window. As the Hanning window is used in this research, (7) yields,

$$\delta=\frac{2-r}{1+r} \quad (8)$$

The algorithm assumes that the spreading of two close frequency harmonics will not overlap, since then the value of $\max(v_{i+1}, v_{i-1})$ will be subject to error. This error can be reduced by decreasing f_{res} which decreases the spectral leakage.

2.2 Estimation of phase position

Only with the vertical vibration signal, it is impossible to find the position of the imbalance easily. Therefore, the time reference signal is also used. After low pass filtering and down-sampling, the two signals are sine-wave signals with the same frequency, which is equal to the rotor rotation speed. There is a phase lag between the vibration signal and time signal according to the position of the imbalance on the rotor. By calculating the phase lag, it is possible to determine the phase position of the imbalance with the reference point. A Lissajous diagram algorithm (Su and Chong, 2004) is implemented to compute the phase lag.

The Lissajous diagram is a basic approach to determine the relative characteristics of two sources, primarily their frequency and phase relations. By applying two signals as vertical axis (y axis) and horizontal axis (x axis) inputs, an ellipse trace can be obtained, except for cases where the phase lag is a multiple of $\pi/2$. From the ellipse curve, the phase lag between two inputs can be obtained as,

$$\sin\phi=\frac{y-\text{intercept}}{y-\text{amplitude}}=\frac{y_1}{y_2} \quad (9)$$

where ϕ is the phase lag between two signal ($0<\phi<\pi/2$), y_i is the value where x is 0 and y_2 is the max value of magnitude.

The time signal is set as horizontal input (x input) while the vibration signal is vertical input (y input). The mean value of time signal is removed to make the time signal a sine wave signal on axis. The intercept value and amplitude value of the vibration periodical signal are obtained statistically. The y axis intercept value is obtained as,

$$y_1=\frac{1}{N}\sum_{n=1}^{N}V_{intercept} \quad (10)$$

where N is the number of periods of the vibration signal, $V_{intercept}$ is the magnitude value of each period where time signal magnitude is 0. And the y axis amplitude value is obtained as,

$$y_2=\frac{1}{N}\sum_{n=1}^{N}V_{amplitude} \quad (11)$$

where N is the number of period of vibration signal, $V_{amplitude}$ is the max value of the magnitude in each period. Thus, the phase lag ϕ can be obtained from y_1 and y_2.

As the original Lissajous diagram only can indicate a phase lag less than π, the new algorithm divides the Lissajous diagram into four segments according to clockwise rotation or counter-clockwise rotation of the diagram. By distinguishing the diagram segment first, the phase lag can be calculated in the 2π range. The algorithm is illustrated in Fig. 2. So the phase lag α of the mass unbalance on the rotor is defined as,

$$\alpha=\begin{cases}\phi & 0\le\alpha<\pi/2\\ \pi-\phi & \pi/2\le\alpha<\pi\\ \pi+\phi & \pi\le\alpha<3\pi/2\\ 2\pi-\phi & 3\pi/2\le\alpha<2\pi\end{cases} \quad (12)$$

where α is the phase lag on the rotor, ϕ is obtained in Eq. (9).

Therefore the phase position of the imbalance on the rotor can be computed according to the phase lag. The geometries of a rotor with imbalance are shown in Fig. 3. First, a zero reference point of the imbalance is defined on the rotor. The α_0 is the phase lag between the zero reference point and time reference point, which is obtained in advance through experiment. Then the calculated position of imbalance would be,

$$\alpha_{MASS}=\alpha-\alpha_0 \tag{13}$$

With the reference of zero reference point, the position of mass unbalance can be located efficiently and accurately through this method.

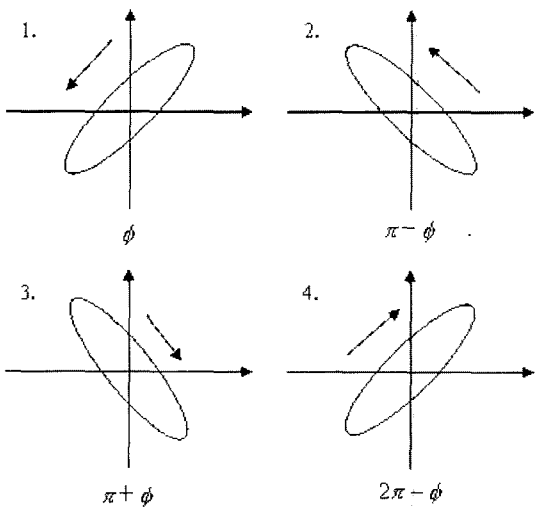

Fig. 2 Phase lag algorithm based on Lissajous Diagram

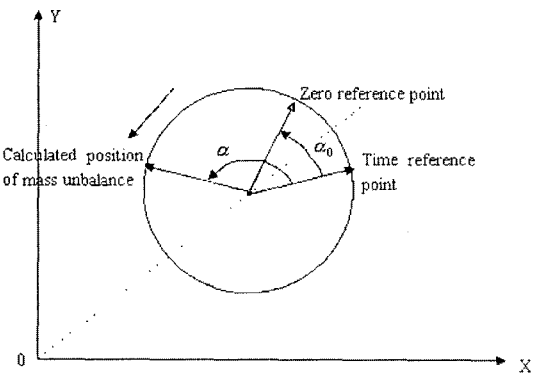

Fig. 3 Geometries of a rotor with unbalance mass

3. Designed DSP System

3.1 Hardware of the DSP system

A block diagram of the designed system for the imbalance analysis is shown in Fig. 4. The system mainly consists of two parts, a host PC for result diagnosis and a DSP for FFT and Lissajous diagram calculation.

The test rig here is a motor and clutch arrangement, which the rotor is driven by a motor through a belt and brought up to a predetermined rpm value for analyze. A pair of piezoelectric sensors are mounted in the pedestal adjacent to and spaced axially along the rotor, and an optical sensor above the rotor, in order to assure an optimum coupling. The structure of the test rig is shown in Fig. 5. The force transducers are coupled mechanically to the shaft and provide periodic electrical output signals indicative of imbalance forces transmitted through the shaft when the rotor is driven rotationally. The reference position of the rotor is monitored with respect to the optical sensor during every rotation.

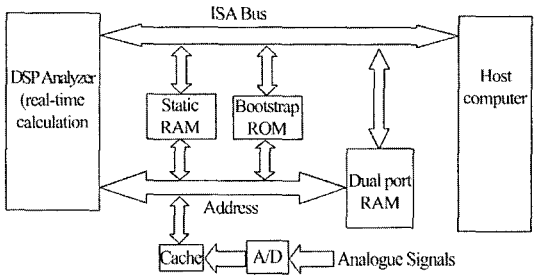

Fig. 4 Block diagram of the DSP-based Imbalance analysis system

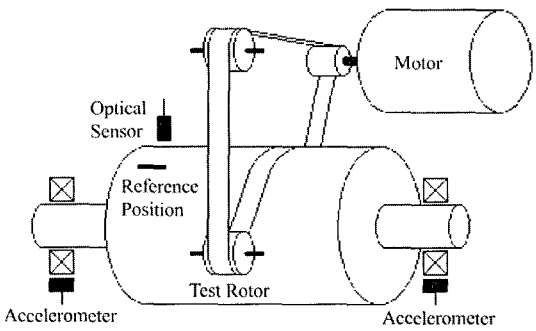

Fig. 5 Structure of the test rig

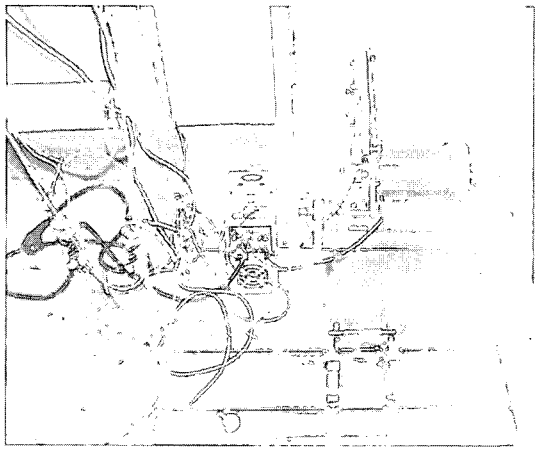

Fig. 6 Picture of the test rig

Fig. 6 shows a picture of the test rig used in this research, all the components can be referred to the structure of the test rig in Fig. 5. The vertical force exhibited by the imbalance and rotation time data are converted to digital form through the use of ADI AD1674 devices for DSP processing.

A Texas Instruments TMS320C32 DSP chip is used for real-time analysis. The chip architectures, featuring multiple buses, provide a high degree of parallelism. It can perform parallel multiply and add operations in integer or floating point data in a single clock cycle. In this system, the TMS320C32 is running at its maximum clock speed, yielding a maximum throughput of 40 MFLOPS to ensure real-time analysis. The C compiler supplied by Texas Instruments generates efficient object code, using the parallel instructions of the TMS320C32 assembly language source code, making it easy to optimize critical sections of the code. Also included is a debugging environment, which supports multiple source files and multiple watch variables, including auto-variables (Kumbla et al., 1995). The designed DSP board is shown in Fig. 7.

The TMS320C32 has two memory buses, the primary bus and the expansion bus. On the primary bus the board has static RAM and Bootstrap ROM on the board. The data can be transferred in either 16 bit or 8 bit mode. The memory on the primary bus is dual ported with host PC. Transfers can be either under CPU, interrupt or

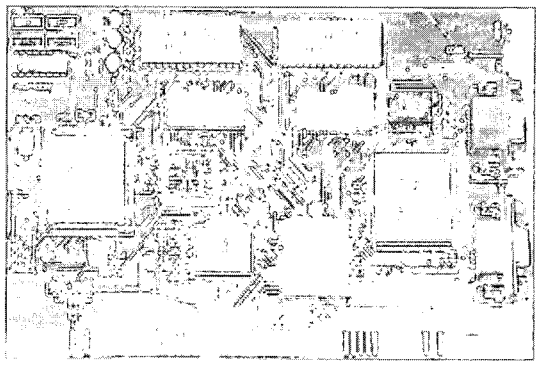

Fig. 7 Designed DSP board

DMA control, or any combination of the three. The host interface is designed so that the board can reside on the bus for multi-processing application since this system has performed real-time analysis. The TMS320C32 has two on-chip serial channels for 8/16/32 bit transfers of up to 8.3 Mbps (Kumbla et al., 1995; Zhou et al., 2001; 2001; Xu et al., 2002). The board has two A/D converters featuring 12 bit resolution connected to analogue signals input and communicates with host PC by dual port RAM via ISA bus.

3.2 The software of the DSP system

Dedicated software is developed to feature the previously described DSP system with imbalance estimation capabilities. It can be subdivided into three main procedures corresponding to the three steps needed to achieve a real-time imbalance analysis: i) signal processing for de-noising, ii) imbalance estimation, and iii) phase position estimation. The software structure of the DSP system is schematized in Fig. 8. All of these procedures have been implemented on the DSP in order to optimize the response time.

The signal processing software, executed by the DSP, analyzes the vibration signal in time domain and de-noises the signal for proper analysis. The sampling frequency is set at 10800 Hz to avoid aliasing. Theoretically, only the characteristic frequency on rotation speed corresponds to the imbalance (Chow and Hai, 2004), thus, to improve the frequency resolution and eliminate the noise, the raw signal is filtered according to the test rotation speed and decimated with a

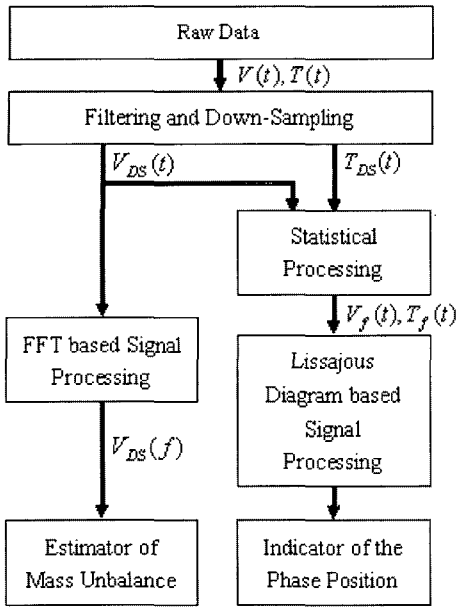

Fig. 8 Software structure of the DSP-based imbalance analysis system

decimation factor equal to 10. The signal processing step of the software performs the two operations in a single step, allowing a meaningful reduction of the computational load. The so-obtained sample sequence is windowed in 1080 points.

Each time the signal processing procedure is completed, the spectrum of the vibration signal is obtained through FFT. The chosen characteristic amplitude on rotation speed of the measured spectrum is compared with the reference unit amplitude, with the aim of estimating the mass unbalance. The high variability in successive measurements, carried out in different test speeds (360-2160 rpm), suggests the use of a statistical approach for defining the reference unit amplitude. The DSP executes this mass imbalance estimation procedure, taking about 0.01 ms.

The efficient phase position estimation for the imbalance on the rotor is realized through the combined use of vibration signal and time reference signal, which are also obtained from signal processing step. The new Lissajous diagram (Su and Chong, 2004) is directly implemented on the DSP, in order to obtain better time performance. First the checks on the vibration signal and time signal are performed, to find the $V_{intercept}$ and $V_{amplitude}$ in each period of the vibration signal as well as the Lissajous diagram form it belongs to. Then, the mean intercept and amplitude is generated with the statistical processing to calculate the phase lag between vibration signal and time reference signal. The phase position of the imbalance is finally estimated by comparing the phase lag with the reference point.

The analysis result is passed through the DSP to the host computer, and the output of the software is the exact mass imbalance and its phase position. The DSP system executes those three procedures with about 0.02 ms.

4. Experimental Evaluation of the System

As for the performance evaluation, in terms of diagnostic capabilities and response time, of the designed system, several experimental tests using the described test rig are carried out. The accuracy and efficiency are evaluated by comparing the analysis results with the theoretical values and the response time. The experiment is conducted at Network System Control Lab., Chonbuk National University, under the auspices of Korean Power Electric Company. The structure and experimental system of the test rig are shown in Figs. 5~6. In order to provide a higher resolution in the sampled signal, totally seventy-five groups of time-independent data are used in this research with a sampling rate of 10800 Hz.

Both the balance condition and several imbalance conditions are tested in this research. The imbalance conditions on the rotor are set to 1g, 2.1g and 3.2g in single position and two separate 1g in adjacent positions, respectively. The phase between the separate 1g imbalance is 45 degrees. The sixty 1g tests are used to define the unit mass amplitude M_{UNIT} statistically. A summary of the test cases used to evaluate the performance of the designed DSP system is given in Table 1. The vibration signals of both balance and imbalance conditions are illustrated in Fig. 9. The test speed is 1080 rpm and after the processing of the DSP, Fig. 10 depicts the corresponding

Table 1 Summary of analyzed imbalance experiments

Test Condition	Number of Cases	Detailed Description
Balance	15	Balance rig
Imbalance	60	Imbalance mass : 1, 2.1, 3.2, 1×2g 15 test speed 360 rpm 15 test speed 1080 rpm 15 test speed 1800 rpm
Total cases	75	

Table 2 Results of the balancing system

Theoretical Value	2.1g	3.2g	1g×2
Test speed 360 rpm	2.0693g	3.0427g	1.9479g
Test speed 1080 rpm	2.1776g	3.3205g	1.9556g
Test speed 1800 rpm	2.2671g	3.3887g	1.9637g
Average error %	3.39	1.58	2.21
Effectiveness %	98.2		

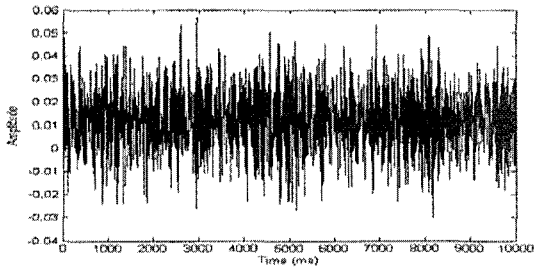

(a)

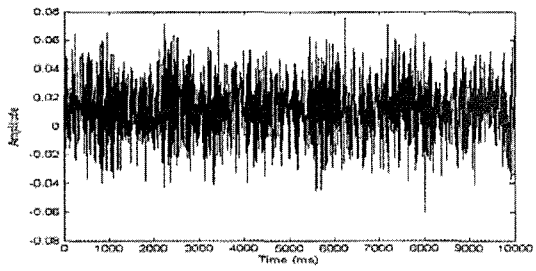

(b)

Fig. 9 Vibration signals at a test speed of 1080 rpm (a) balancing condition (b) imbalance condition

magnitude spectra in the 0~270 Hz frequency range. The estimation results of imbalance conditions through test speed 360~1800 rpm are listed in Table 2. Checked with theoretical values, we

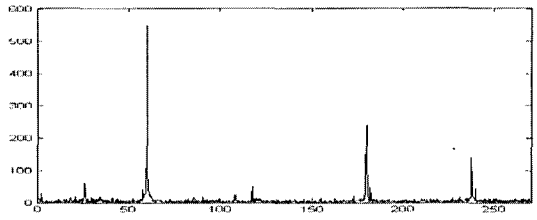

(a)

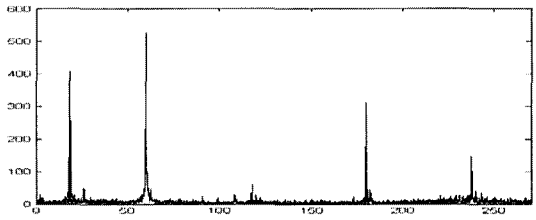

(b)

Fig. 10 (a) Magnitude spectrum in 0-270 Hz frequency range for balance condition at a test speed of 1080 rpm (b) Magnitude spectra in 0-270 Hz frequency range for imbalance conditions at a test speed of 1080 rpm

can find that the DSP-based system has a reliable performance for detecting the weight of imbalance. The convergence weight of the two separate 1g mass imbalance between 45 degree is also estimated accurately, which proves that the convergence conditions are always satisfied, and this method can be used to balance the imbalance rotor practically.

Also the phase position is estimated and analyzed under different imbalance conditions and different positions in the proposed DSP system. The outputs of the numerical results are shown in Tables 3~5, and compared in Figs. 11 and 12. The difference between the first two cases is the imbalance distribution on the rotor, and the two separate 1g apart from 45 degrees is tested in the last case, which the convergence position is calculated. The comparison between the test position and the calculated result demonstrates accurate estimation of the proposed system. The designed system is more advanced, as the exact phase position is told instead of the indication of such a subsystem or boundary by the former system.

The effectiveness of the proposed DSP-based imbalance diagnosis system is explored through experimental tests under different imbalance mass

Table 3 The Numerical results of Case 1

Test Speed : 1080 rpm	Position	Result	Error %
Imbalance : 2.1g	45°	44.4862°	0.14
	90°	89.7250°	0.07
	135°	133.4967°	0.42
	180°	180.8455°	0.23
	225°	225.0710°	0.01
	270°	272.2947°	0.63
	315°	317.6273°	0.72

Table 4 The Numerical results of Case 2

Test Speed : 1080 rpm	Position	Result	Error %
Imbalance : 3.2g	45°	45.1763°	0.04
	90°	91.1052°	0.31
	135°	134.4712°	0.14
	180°	179.4582°	0.15
	225°	224.0198°	0.27
	270°	271.8361°	0.51
	315°	315.2639°	0.07

Table 5 The Numerical results of Case 3

Test Speed : 1080 rpm	Convergence Position	Result	Error %
Imbalance : 1g×2	22.5°	24.3516°	0.51
	67.5°	65.0633°	0.67
	112.5°	110.5712°	0.53
	157.5°	156.0006°	0.41
	202.5°	200.9603°	0.42
	247.5°	247.8419°	0.09
	292.5°	294.5738°	0.57
	337.5°	339.1405°	0.45

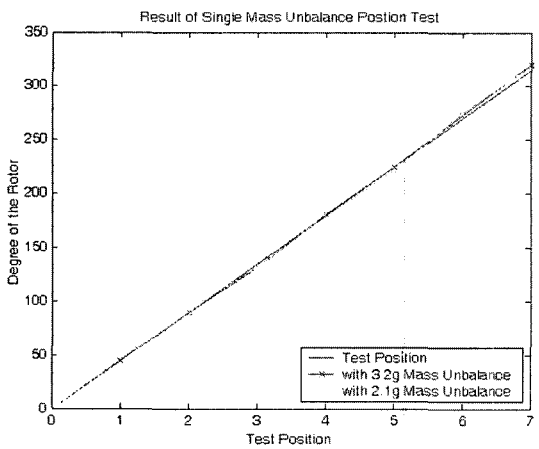

Fig. 11 Comparison of single imbalance position results

and position conditions. We can find that the proposed system is capable of identifying the imbalance efficiently and effectively. There is some small error in estimation due to the noise included in the vibration signals and the imbalance used in this study is very small compared with the test rig. All cases of imbalance have been successfully estimated in this study.

In general, balancing is effected by adding weights or digging holes at given radial distances from the axis of rotation. The test rig is considered to investigate the effectiveness of balancing. The simulation result of balancing is shown in Fig. 13. From this figure, we find that the peak

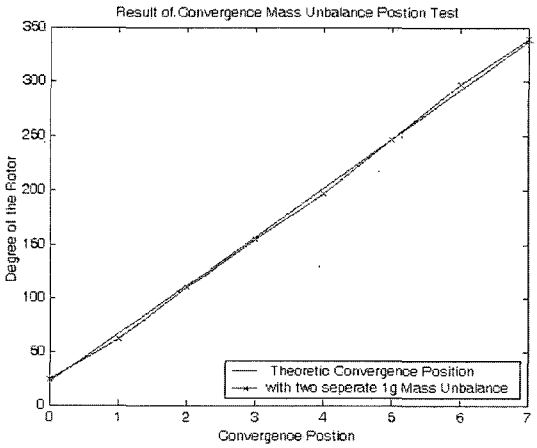

Fig. 12 Comparison of convergence imbalance position result

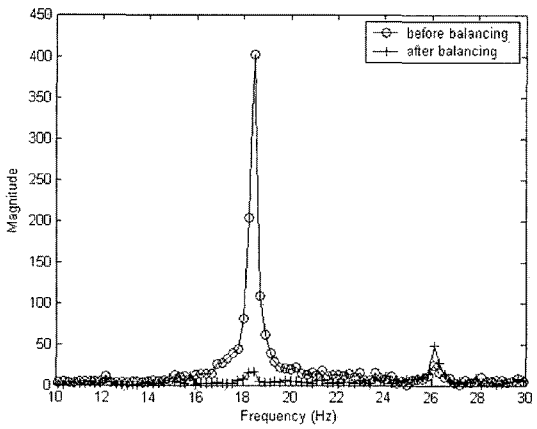

Fig. 13 Comparison of Magnitude of before and after balancing in 3.2g imbalance condition at test speed 1080 rpm

response in 3.2g imbalance is about 4.11% of the original response before balancing. So the proposed DSP-based imbalance analysis system is a practical and effective way to balance imbalance rotors.

A mean delay of 300 ms for imbalance analysis is measured in the DSP system after the starting of data input, resulting in the agreement with the real-time analyzing realized by the proposed DSP system.

5. Conclusions

In the present paper a DSP-based real-time imbalance analysis system is described for the imbalance analysis of rotation machine. It allows imbalance monitoring to be carried out on-line, with a consequent increase in the system and in environmental safety.

Based on FFT and Lissajous diagram, the weight and phase position of imbalance is identified by the proposed system. The above DSP-base system provides a practical way to solve the imbalance problem of the rotating machine. The use of the statistical method reduces the computation time and increases the accuracy. Theoretical results have been given. Several examples are illustrated and compared to verify the proposed system. The applicability of the proposed system is shown through the examples.

The proposed system is very effective due to the facts that it can be applied to most imbalance rotor systems and can be extended to numerous application fields. It may be a new means for achieving a more precise balance in actual systems in the future.

References

Bishop, R. E. D. and Gladwell, G. M. L., 1959, "The Vibration and Balancing of an Unbalanced Rotor," *Journal of Mechanical Engineering Science*, pp. 66~77.

Blasco, G. R., Asher, G. M., Sumner, M. and Bradley, K. J., 1996, "Performance of FFT-Rotor Slot Harmonic Speed Detector for Sensorless Induction Motor Drives," IEE Proc. Electr. Power Appl., Vol. 143, No. 3, pp. 258~268.

Choi, M. S., 2003, "Free Vibration Analysis of Plate Structures Using Finite Element-Transfer Stiffness Coefficient Method," *KSME International Journal*, Vol. 17, No. 6, pp. 805~815.

Chow, T. W. S. and Hai, S., 2004, "Induction Machine Fault Diagnostic Analysis with Wavelet Technique," *IEEE Trans. on industrial electronics*, Vol. 51, No. 3.

Enrich, F. F., 1987, "Two Plane Balancing of a Rotor System Without Phase Response Measurements," *ASME Journal of Vibration, Acoustics*, Stress and Reliability in Design, 109 pp. 162~167.

Hoextermann, E., 1988, "Erfahrung Mit Schaeden in form von Anrissen und Bruecken an Dampfturbienenwellen, Radscheiben und Generatorlaufen," *VGB Technische — Wissenschaftliche Berichte Waermekraftwerke*, VGW-TW 107.

Hong, S. H. and Seo, Y. G., 2001, "A Study on the Synchronous Response of General Rotor-Bearing Systems due to Initial Deformation," *KSME International Journal*, Vol. 15, No. 9, pp. 1226~1239.

Hong, S. W. and Park, J. H., 1997, "An Efficient Method for the Unbalance Response Analysis of Rotor-Bearing Systems," *Journal of Sound and Vibration*, 200(4) pp. 491~504.

Kim, S. K. and Yoo, H. H., 2002, "Vibration Analysis of Rotating Composite Cantilever Plates," *KSME International Journal*, Vol. 16, No. 3, pp. 320~326.

Kim, W. K., Kim, J. T. and Kim, J. S., 2003, "Development of a Criterion for Efficient Numerical Calculation of Structural Vibration Responses," *KSME International Journal*, Vol. 17, No. 8, pp. 1148~1155.

Kumbla, K. K., Mohammad-R., Akbarzadeh-T. and Jamshidi, M., 1995, "TMS320 DSP Based Neuro-Fuzzy Controller," *Systems, Man and Cybernetics, 1995. 'Intelligent Systems for the 21st Century'., IEEE International Conference on*, Vol. 5, pp. 4015~4020.

Park, J. T. and Choi, N. S., 2004, "Flexural Vibration Analysis of a Sandwich Beam Specimen with a Partially Inserted Viscoelastic Layer," *KSME International Journal*, Vol. 18, No.

3, pp. 347~356.

Park, R. W., 2000, "Estimation of a Mass Unbalance Under the Crack on the Rotating Shaft," *ICASE.*, Vol. 2, No. 4.

Saito, S. and Azuma, T., 1964, "Balancing of Flexible Rotors by the Complex Modal Method," *ASME Journal of Vibration, Series B*, 86(3) pp. 273~279.

Shimada, K. and Miwa, S., 1980, "Balancing of a Flexible Rotor," Bulletin of the JSME, 23(180) pp. 938~944.

Shin, G. O. Y. and Lee, A., 1997, "Identification of the Unbalance Distribution in Flexible Rotors," *Int. J. Mech. Sci.*, Vol. 39. No. 7., pp. 841~857.

Su, Hua and Chong, K. T., 2004, "An Efficient Method for the Mass Unbalance Analysis of a Rotor System Using FFT and Lissajous Diagram," in *2004 International Conference of Control, Automation and Systems*, Bangkok, Thailand.

Tahk, K. M. and Shin, K. H., 2002, "A Study on the Fault Diagnosis of Roller-Shape Using Frequency Analysis of Tension Signals and Artificial Neural Networks Based Approach in a Web Transport System," *KSME International Journal*, Vol. 16, No. 12, pp. 1604~1612.

Wylie, C. R. and Barrett, L. C., 1982, *Advanced Engineering Mathematics*, McGraw-Hill.

Xu, H. S., Toliyat, H. A. and Petersen, L. J., 2002, "Five-Phase Induction Motor Drives with DSP-Based Control System," *Power Electronics, IEEE Transactions on*, Vol. 17, Issue. 4, pp. 524~533.

Zhou, J. S., Liu, Z. Y. and Pei, R., 2001, "A New Nonlinear Model Predictive Control Scheme for Discrete-Time System Based on Sliding Mode Control," *American Control Conference, 2001. Proceedings of the 2001*, Vol. 4, pp. 3079~3084. Texas Instruments TMS320C3X User's Guide 2001.